

# AN ACCURATE METHOD OF ASSESSING TUBE WALL THICKNESS BASED ON FLOW BOILING AND SINGLE PHASE HEAT TRANSFER MEASUREMENTS

A. Tanase<sup>\*</sup>, D.C. Groeneveld<sup>†\*</sup>

<sup>\*</sup>University of Ottawa, Ottawa, ON Canada K1N 6N5

<sup>†</sup>Atomic Energy of Canada Limited, Chalk River, ON Canada K0J 1J0

## Abstract

Fuel bundle simulators used in thermalhydraulic studies typically consists of bundles of directly heated tubes. It is usually assumed that these tubes have a uniform circumferential heat flux distribution. In practice, this heat flux distribution is not uniform because of wall thickness variations. Ignoring the non-uniformity in wall thickness will lead to underestimating the critical heat flux and overestimating the film boiling temperature.

It is the objective of this paper to present an accurate method for determining this wall thickness variation. The method is based on the principle that for directly heated tubes, cooled internally, the single phase heat transfer coefficient (or the wall superheat in nucleate boiling or at ONB) is uniform around the circumference and is therefore independent of the variation in wall thickness.

Three analytical methods for evaluating the wall thickness variation have been compared:

- based on single phase heat transfer data,
- based on nucleate boiling data,
- based on ONB data

The wall thickness evaluations have subsequently been validated by two direct measurements: (i) based on direct caliper measurements, and (ii) based on photographic measurements

The agreement between these five methods is good. The results show that the proposed analytical approach is a highly accurate method for determining the circumferential wall thickness variation.

## 1. Introduction

The method for determining the circumferential wall thickness variation presented in this paper is based on the measurement of the non-uniformity in circumferential wall temperature distribution. The accuracy of the estimated wall thickness variation depends strongly on the accuracy of the surface temperature measurement. In this paper we will therefore first describe a method for calibrating the thermocouples used to measure the surface temperature of a direct current (DC) heated tube and for detecting the geometrical asymmetries (eccentricity, variation of

tube radii) at the location of thermocouples. The method can be effectively used for estimating the local tube wall thickness (at the middle of the tube for example) from measurement of inside and outside tube radii at the end of the tube and the assumption that their variation is negligible along the tube length.

### 1.1 Experimental setup

The test section used for current experiment is an Inconel 600 tube having heated length  $L_h=2\text{m}$  and measured inside diameter  $D_i=5.585\pm0.0013\text{ mm}$  and outside diameter  $D_o=8.020\pm0.0013\text{ mm}$ . The test section is cooled internally and equipped on the outside with three pairs of K-type thermocouples. They are located at opposite sides at three axial locations of the test section, as shown in Figure 1.

Ideally, the thermocouple pairs located at the same axial location (such as thermocouple 1 and thermocouple 2) should indicate the same temperature. The expected uncertainty in the thermocouple readings is  $0.4\text{ }^\circ\text{C}$  [4], i.e. we are 95% confident that replacing any thermocouple with a similar type the difference between the measurement and the true temperature is less than  $0.4\text{ }^\circ\text{C}$ . This uncertainty can be reduced for a given thermocouple using appropriate calibrations. In order to quantify the thermocouple inaccuracy, several tests were performed.

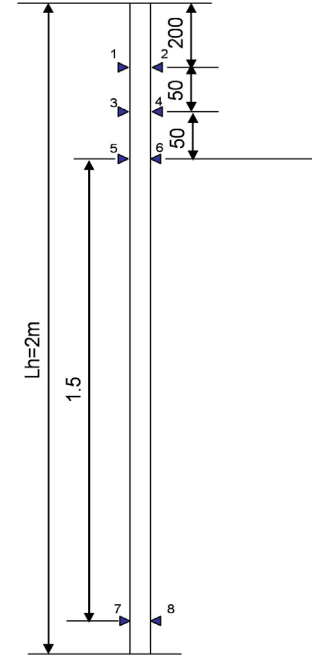


**Figure 1** Test section and thermocouple axial positions

### 1.2 Thermocouple calibration

The thermocouple calibrations were performed by circulating single phase coolant through the test section using several bulk coolant temperatures. Because no heating is applied to the test section, wall thickness variation do not affect the readings. If the coolant temperature is close to the ambient temperature and/or the test section is thermally insulated, then heat losses and contact resistance effects are minimized or non-existent. Therefore, this test will show the inaccuracies (random and systematic) of the thermocouples and the analog-digital conversion (ADC) but for a relatively narrow range of temperatures.

Note that the calibrations were performed at high mass flux ( $G=3500\text{ kgm}^{-2}\text{s}^{-1}$ ) and at pressure approximately equal with 2380 kPa. The reference bulk coolant temperature is based on the averaged values from resistance temperature detectors (RTD's) located at the inlet and outlet of the test section. Thermocouple voltage outputs were converted into temperatures based on standard tables for type-K thermocouples. Table 1 shows the averaged "error" values for all thermocouples

The general form of the correction function is  $\Delta T = aT + b$ . Table 2 gives the optimized coefficients  $a$  and  $b$ . The correction is performed as  $T_{\text{corrected}} = T_{\text{raw}} - (aT_{\text{raw}} + b)$ .

**Table 1** Average difference (K) between measured thermocouple temperature and the reference temperature ( $T_{ref}$ )

$T_{ref}$ (°C)	$T_{wo1}$	$T_{wo2}$	$T_{wo3}$	$T_{wo4}$	$T_{wo5}$	$T_{wo6}$
10	0.16	0.19	0.04	-0.05	0.06	-0.05
20	0.21	0.14	0.07	-0.01	-0.01	-0.03
30	0.16	0.11	0.04	-0.01	0.02	0.00
40	0.28	0.21	0.15	0.07	-0.02	-0.01
50	0.23	0.11	0.06	-0.02	-0.13	-0.08
60	0.19	0.02	0.05	-0.08	-0.20	-0.03
70	0.07	-0.09	-0.08	-0.12	-0.35	-0.12
80	0.12	-0.19	0.13	-0.17	-0.28	0.18

**Table 2** Coefficients of the 1<sup>st</sup> degree calibration polynomials

	TC1	TC2	TC3	TC4	TC5	TC6
<b>a</b>	0.0016	-0.0008	0.0017	0.0012	-0.0033	-0.0001
<b>b</b>	0.1069	0.126	-0.0347	-0.1087	0.0119	-0.0975

Using the correction functions will result in more uniform temperature distribution (smaller difference between thermocouple readings) for single phase and zero heat flux, which is closer to the ideal situation where all thermocouple measurements are equal.

The insulation of the test section minimizes heat loss. Previous tests have shown that at ~ 60 °C the insulated test section has a higher surface temperature (~0.63 °C) compared with un-insulated test section. Table 3 shows the difference between averaged RTD and averaged thermocouple at different fluid temperatures, for the insulated test section.

**Table 3** Difference between averaged RTD measurement and averaged thermocouple measurements

$T_{ref}$ (°C)	10	20	30	40	50	60	70	80
$T_{RTD} - T_{TC}$ (K)	-0.06	-0.06	0.00	-0.11	-0.03	0.01	0.15	0.10

Note that at temperatures higher than 60 °C the RTDs indicate a systematically higher temperature than the thermocouples, suggesting that that heat losses may decrease the thermocouple temperature readings by 0.1-0.15 °C.

## 2. Circumferential temperature variation in eccentric heated tubes

Tubes used in heat transfer experiments have some circumferential variation in wall thickness, which result in small temperature variations between thermocouples located at the same axial position, but different circumferential position. This wall thickness variation is usually due to a slight eccentricity of the outside diameter w.r.t. the inside test section diameter.

In order to assess the effects of this asymmetry, a simple geometrical analysis of eccentricity has been performed (see Figure 2).

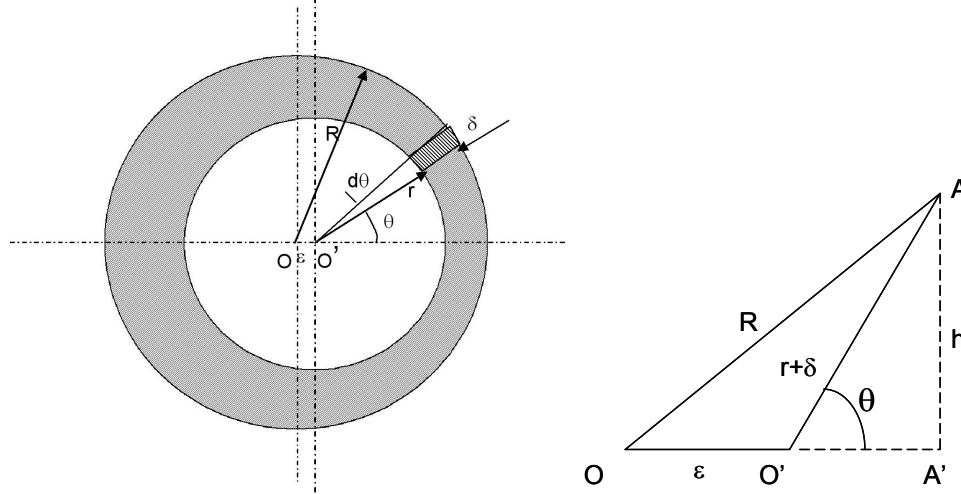


**Figure 2** Test section eccentricity

If the outside radius of a test section is  $R$  and the inside radius is  $r$ , in the ideal situation the both circles are concentric so the wall thickness ( $\delta$ ) is the same regardless the circumferential position (angle  $\theta$ ). For a small eccentricity  $\varepsilon$  (defined as the distance between the centers of inside and outside circles), the wall thickness varies with  $\theta$ . The wall thickness can then be expressed as a function of  $R$ ,  $r$  and  $\theta$ . Considering the triangle  $OO'A$ , where  $O$  is the center of circle with radius  $R$  and  $O'$  is the centre of the circle with radius  $r$  and  $A$  is an arbitrary point on the test section surface angular coordinate  $\theta$  and applying Pythagora theorem, we have:

$$(\varepsilon + O'A')^2 + h^2 = R^2 \quad (1)$$

$$O'A' = (r + \delta) \cos \theta \quad (2)$$

$$h = (r + \delta) \sin \theta \quad (3)$$

Combining Eq. (1) (2) and (3) and solving for  $\delta$  we obtain:

$$\delta = \sqrt{R^2 - (\varepsilon \sin \theta)^2} - \varepsilon \cos \theta - r \quad (4)$$

Indeed, checking the wall thickness at some particular points where it is known (such as  $\theta = 0$  or  $180$  deg) we obtain  $\delta = R - \varepsilon - r$  and  $\delta = R + \varepsilon - r$  which confirms the correctness of eq. 4.

For very small eccentricities (one order of magnitude less than  $r$ ,  $\varepsilon < 0.5$  mm) the product  $(\varepsilon \sin \theta)^2$  can be neglected, hence the expression of wall thickness is simplified as:

$$\delta = R - r - \varepsilon \cos \theta \quad (5)$$

Assuming that the geometry parameters and material properties do not change in axial direction of the test section, the voltage applied to it is  $U$  and the electric resistivity is  $\rho$ , the volumetric heat source is:

$$dq_v = \frac{dP}{dV} = \frac{U^2}{\rho L^2} \quad (6)$$

The surface heat flux is:

$$q_s = q_v \left( \frac{R+r}{2r} \right) \delta = \frac{U^2}{\rho L} \left( \frac{R+r}{2r} \right) \delta \quad (7)$$

From equations (6) and (7) it can be seen that the local surface heat flux ( $q_s$ ) is proportional to the local wall thickness  $\delta$  but the volumetric heat generation rate  $q_v$  is independent of wall thickness. Because of proportional relation between  $q_s$  and  $\delta$ , a variation of few percent in wall thickness (3-4% are typical values) will results in practically the same variation in the surface heat flux. This is detected by slightly different readings of thermocouple located at the same axial position, but at different angles. The difference between thermocouple readings will increase with the heat flux.

Another factor that may influence the local surface heat flux is the non-uniformity in the material composition which may results in a non-uniformity in thermal conductivity and electrical resistivity. This additional uncertainty is considered negligible compared to the impact of a typical 3-4% variation in wall thickness

The heat conduction equation for a tubular geometry with internal heat sources and neglecting heat loss, is:

$$T_{wi} - T_{wo} = (R^2 - r^2) \frac{q_v}{4k} - \frac{q_v R^2}{2k} \ln \frac{R}{r} \quad (8)$$

or, as a function of wall thickness ( $\delta$ ),

$$T_{wi} - T_{wo} = (R+r) \cdot \delta \frac{q_v}{4k} - \frac{q_v R^2}{2k} \ln \frac{R}{r} \quad (9)$$

The wall temperature drop can be expressed as a function of outside tube radius  $R$  and tube wall thickness  $\delta$  :

$$\Delta T_w = \frac{q_v(R^2 - r^2)}{4k} - \frac{q_v R^2}{2k} \ln \frac{R}{r} = \frac{q_v(R+r)(R-r)}{4k} - \frac{q_v R^2}{2k} \ln \frac{R}{R-\delta} \quad (10)$$

$$\Delta T_w(\delta) = \frac{q_v(2R - \delta)\delta}{4k} - \frac{q_v R^2}{2k} \ln \frac{R}{R - \delta} \quad (11)$$

The temperature difference between two thermocouples located at different circumferential positions (but the same axial location)  $\Delta T_{wo}$ , having local wall thickness  $\delta_1$  and  $\delta_2$  respectively is given by:

$$\Delta T_{wo} = \frac{q_v R^2}{2k} \ln \frac{R - \delta_2}{R - \delta_1} + \frac{q_v}{4k} [2R(\delta_2 - \delta_1) + (\delta_1 - \delta_2)(\delta_1 + \delta_2)] \quad (13)$$

If we assume that  $\delta_1$  and  $\delta_2$  are located at the opposite side of the test section ( $180^\circ$  apart) then average between  $\delta_1$  and  $\delta_2$  is the nominal wall thickness  $\delta_0$ :

$$\delta_0 = \frac{\delta_1 + \delta_2}{2} \quad (14)$$

Solving equations (13) and (14) we can find the unknown  $\delta_1$  and  $\delta_2$ , respectively. Experimental measurements performed to determine outside wall temperatures at different heat fluxes are shown in Table 4 and graphically in Figure 3:

**Table 4** Corrected outside wall temperatures as function of averaged surface heat flux

$q_s$ , $\text{kWm}^{-2}$	$q_v$ , $\text{kWm}^{-3}$	$T_{wo1}$ $^{\circ}\text{C}$	$T_{wo2}$ $^{\circ}\text{C}$	$T_{wo3}$ $^{\circ}\text{C}$	$T_{wo4}$ $^{\circ}\text{C}$	$T_{wo5}$ $^{\circ}\text{C}$	$T_{wo6}$ $^{\circ}\text{C}$	Observations
151.57	102210	80.92	77.15	79.28	75.35	77.42	73.72	Single phase
154.78	104380	82.24	78.43	80.69	76.56	78.76	74.94	
156.49	105530	82.96	79.10	81.40	77.42	79.53	75.61	
158.12	106630	83.68	79.72	81.86	77.98	80.12	76.11	
159.78	107750	84.32	80.37	82.61	78.59	80.79	76.87	
161.44	108870	83.38	81.04	83.38	79.31	81.46	77.54	
165.18	111390	83.81	81.92	83.48	80.74	83.04	79.01	
166.37	112190	84.00	82.20	83.71	81.07	83.55	79.49	
167.89	113220	84.05	82.40	83.79	81.45	84.12	80.09	
171.22	115460	84.24	82.71	84.07	82.34	83.91	81.08	
174.17	117450	84.52	83.04	84.37	82.70	84.08	81.94	
176.59	119080	84.63	83.17	84.45	82.95	84.30	82.38	
178.09	120100	84.76	83.38	84.55	83.07	84.41	82.63	
181.12	122140	84.98	83.51	84.86	83.41	84.72	82.99	
185.94	125390	85.22	83.84	85.14	83.65	84.96	83.33	
190.28	128320	85.43	84.13	85.28	83.85	85.18	83.67	
195.71	131980	85.82	84.33	85.61	84.21	85.50	83.99	Fully developed nucleate boiling
205.97	138900	86.45	84.89	86.24	84.82	86.15	84.63	
225.82	152280	87.75	86.09	87.46	85.82	87.38	85.59	

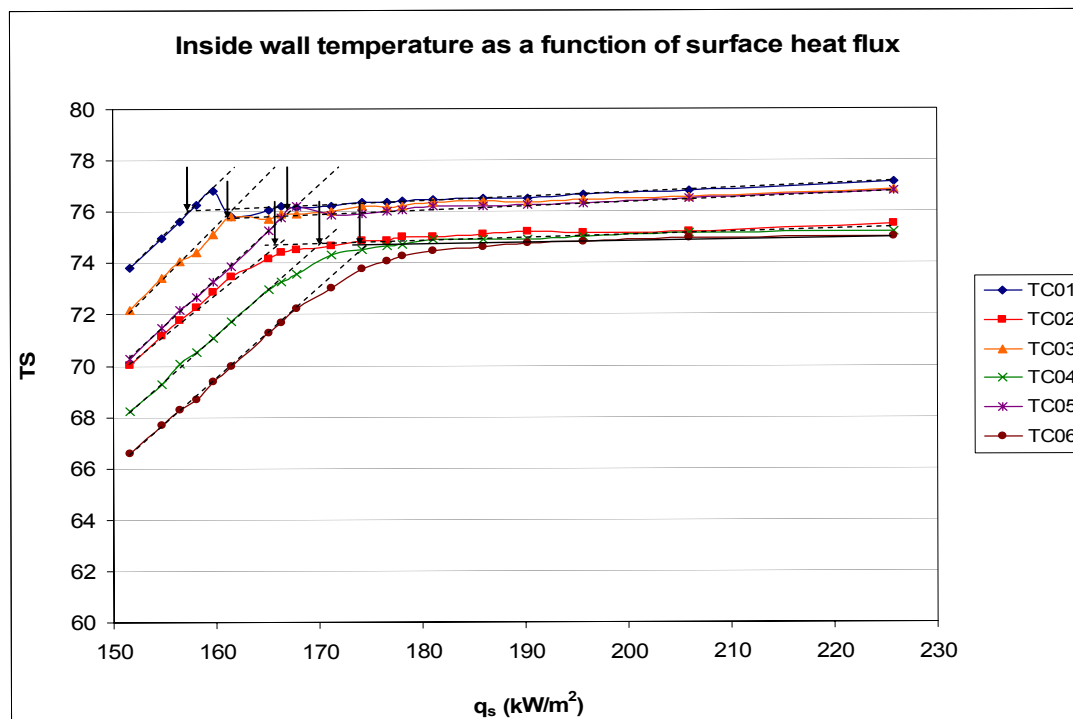


**Figure 3** *Corrected inside wall temperatures as function of averaged surface heat flux*  
**3. Estimation of wall thickness using fully developed nucleate boiling**

The last three rows of Table 4 were considered representative of fully developed nucleate boiling; therefore they were used for estimating of wall thickness:

**Table 5** *Average  $q_s$ ,  $q_v$ , nominal  $\Delta T$  across the wall, wall conductivity and outside measured temperature for fully developed nucleate boiling*

$q_s$ , $\text{kWm}^{-2}$	$q_v$ , $\text{kWm}^{-3}$	$\Delta T_0$ K	$K$ , $\text{Wm}^{-1}\text{K}^{-1}$	$T_{wo1}$ $^{\circ}\text{C}$	$T_{wo2}$ $^{\circ}\text{C}$	$T_{wo3}$ $^{\circ}\text{C}$	$T_{wo4}$ $^{\circ}\text{C}$	$T_{wo5}$ $^{\circ}\text{C}$	$T_{wo6}$ $^{\circ}\text{C}$
195.71	131980	8.01	13.815	85.82	84.33	85.61	84.21	85.50	83.99
205.97	138900	8.43	13.819	86.45	84.89	86.24	84.82	86.15	84.63
225.82	152280	9.24	13.825	87.75	86.09	87.46	85.82	87.38	85.59

Starting from Table 5 and taking the nominal wall temperature drop ( $\Delta T_0$ ) corresponding to nominal wall thickness ( $\delta_0$ ) one can estimate the inside wall surface temperature  $T_{wi}$ . For the current experiment the wall inside temperature for each thermocouple location is calculated in Table 6 as  $T_{woi} - \Delta T_0$ ,  $i=1$  to 6:

**Table 6** *Estimated inside wall temperature ( $^{\circ}\text{C}$ ), for nominal conditions (no eccentricity)*

$q_s$ , $\text{kWm}^{-2}$	$q_v$ , $\text{kWm}^{-3}$	$T_{wi1}$ $^{\circ}\text{C}$	$T_{wi2}$ $^{\circ}\text{C}$	$T_{wi3}$ $^{\circ}\text{C}$	$T_{wi4}$ $^{\circ}\text{C}$	$T_{wi5}$ $^{\circ}\text{C}$	$T_{wi6}$ $^{\circ}\text{C}$
195.71	131980	77.81	76.32	77.60	76.20	77.49	75.98
205.97	138900	78.02	76.46	77.81	76.39	77.72	76.20
225.82	152280	78.51	76.85	78.22	76.58	78.14	76.35

Note the systematic difference between even and odd thermocouple value, explained by the wall thickness difference, since during nucleate boiling the difference between inside wall surface temperatures should be much smaller. If at one geometric location (i.e. TC1) the heat flux is increased, the variation of outside surface temperature is given by the variation of temperature drop inside the tube wall plus the increase in the inside wall temperature. Because the wall thickness is generally constant for a given angle, hence the wall temperature drop is proportional to  $q_s$  (or  $q_v$ ) the radial conduction component can be deducted and the inside wall temperature can be estimated. Even if the real inside wall temperature can not be known at this stage, its variation with  $q_s$  can be found with good accuracy.

Eqn. 7 showed that the surface heat flux is proportional to wall thickness; therefore a difference of few percent in wall thickness will produce a similar difference in heat flux. The contribution of this component can be evaluated by calculating the slope  $dT_{wi}/dq_s$  using data from Table 6. The average slope is  $0.018^{\circ}\text{C}/\text{kW}/\text{m}^2$ , therefore a variation of  $10 \text{ kW}/\text{m}^2$  in heat flux (which is roughly 5%) will increase the inside wall temperature on average by  $0.18^{\circ}\text{C}$ , which is much smaller than the corresponding change in temperature drop across the wall. Therefore for the first estimate of wall thickness this may be neglected (this assumption may be not true if the wall thickness is very thin). Using equation (13) and (14) and assuming that the inside wall temperatures are equal (neglecting the influence of wall superheat on heat flux, for the first iteration only) one finds:

**Table 7** First estimation of wall thickness

Position	TC1	TC2	TC3	TC4	TC5	TC6
Thickness [mm]	1.270	1.165	1.267	1.168	1.270	1.165

For the second iteration, the local surface heat flux can be estimated rewriting eq (7) in the following form:

$$q_{sloc} = q_{savg} \frac{\delta}{\delta_0} \quad (15)$$

Using the wall thickness obtained from the first iteration, one can calculate the local surface heat flux using eq (16). The results are shown in Table 8:

**Table 8** Local surface heat flux at 2<sup>nd</sup> iteration

$q_{savg}$ kWm <sup>-2</sup>	Local surface heat flux $q_s$ (kWm <sup>-2</sup> )					
	TC1	TC2	TC3	TC4	TC5	TC6
195.71	204.1	187.2	203.3	187.8	203.5	187.6
205.97	214.9	195.2	213.6	195.7	213.8	195.6
225.82	235.4	216.3	234.8	216.6	235.1	216.5

The difference in surface heat flux between opposite thermocouple and the corresponding difference for the inside wall temperatures (calculated by multiplying the difference in heat fluxes and the average slope 0.018 °C/kWm<sup>-2</sup>) are shown in Table 9:

**Table 9** Difference in heat flux and nucleate boiling temperatures between two opposite sides of test section

$\Delta q = q_1 - q_2$ (kWm <sup>-2</sup> )	$\Delta q = q_3 - q_4$ (kWm <sup>-2</sup> )	$\Delta q = q_5 - q_6$ (kWm <sup>-2</sup> )	$\Delta T_{NB\ 1-2}$ (K)	$\Delta T_{NB\ 3-4}$ (K)	$\Delta T_{NB\ 5-6}$ (K)
16.9	16.1	17.2	0.30	0.29	0.31
17.8	16.1	17.1	0.32	0.29	0.31
19.1	18.7	20.2	0.34	0.34	0.36

As it can be noticed the differences in surface temperatures due to differences in local surface heat flux are relatively small but they can be accounted for in order to achieve a better estimation of wall thickness. For the next iteration the temperature difference due to different heat fluxes at the opposite sides of the tubes is not neglected, but corrected with values estimated in Table 9. Applying the procedure explained above, the final estimation of wall thickness is shown in Table 10 (there is no difference between the 3<sup>rd</sup> and 4<sup>th</sup> iteration):

**Table 10** Third and fourth iteration of wall thickness

Position	TC1	TC2	TC3	TC4	TC5	TC6
Thickness [mm]	1.261	1.174	1.259	1.176	1.262	1.173

#### 4. Estimation of wall thickness using onset of nucleate boiling (ONB)



This method is based on the fact that at the ONB the wall superheat ( $T_{wi}-T_{sat}$ ) is relatively small and can be predicted by empirical correlations (such as Davis and Anderson (1966), see eq. 16). Because the wall superheat is small, even if the correlation is not very accurate, the error in the temperature prediction is also relatively small. The ONB test was performed at system pressure  $P=2386.9$  kPa and  $G=3060$  kgm<sup>-2</sup>s<sup>-1</sup>.

$$q_{wONB} = \frac{k_l h_{fg} \rho_v (\Delta T_w)^2}{8 \sigma T_{sat}} \quad (16)$$

To detect the ONB the power to test section was increased in very small steps and multiple scans were taken at each power level.

If ONB is used to calculate the wall thickness, one should be aware of the fact that the ONB starts towards the end of the heated length and advances upstream as the surface heat flux increases; therefore the ONB heat flux depends on the axial and circumferential location of the thermocouple on the test section. Examining Figure 6 one can notice that first ONB point is found at TC1 - the most downstream and located on the higher heat flux side of the test section. The next ONB is found at the TC2 and TC3, respectively. It can also be noticed that on the even side (2-4-6, lower local heat flux) the sudden wall temperature reduction typical for the ONB is not as obvious as for the odd side (1-3-5). The experimental data for ONB are presented in Table 11:

**Table 11** Onset of nucleate boiling (ONB), corrected wall temperature, predicted wall superheat and wall thickness

Location	TC1	TC2	TC3	TC4	TC5	TC6
$q_{S_{avg}}$ at ONB	157.31	166.37	161.44	171.22	166.37	176.59
$T_{WO}$	83.55	82.35	83.53	82.49	83.70	82.53
$T_{sat}$	75.47	75.46	75.46	75.46	75.47	75.47
$\Delta T_{ONB}$	0.99	1.01	1.00	1.03	1.01	1.04
$T_{WI}$	76.46	76.47	76.46	76.49	76.48	76.51
$\Delta T_{wall}$	7.09	5.88	7.07	6.00	7.22	6.03
$\delta$ (mm)	1.271	1.137	1.255	1.133	1.250	1.12

$T_{WO}$  was corrected by 0.15 °C to compensate heat loss, as explained in Section 1. Unlike other methods, the ONB wall thickness estimation is performed based on wall superheat correlation at each thermocouple location, which requires very accurate estimation of outside wall temperature. For the first iteration a perfectly symmetric (no eccentricity) tube was considered. Knowing the average heat flux and fluid properties, one can estimate the wall superheat at ONB for TC1-TC6. For the second iteration, starting from wall thickness calculated at the previous step and using equation (15),  $q_{sloc}$  is found; with  $q_{sloc}$  we recalculate wall superheat at ONB and find the final value of wall thickness (Table 12):

**Table 12** Second iteration for wall thickness using ONB

Location	TC1	TC2	TC3	TC4	TC5	TC6
$q_{S_{avg}}$ at ONB	157.31	166.37	161.44	171.22	166.37	176.59
$q_{sloc}$ at ONB	163.32	155.37	166.41	159.34	170.81	162.45
$T_{WO}$	83.55	82.35	83.53	82.49	83.70	82.53

T <sub>sat</sub>	75.47	75.46	75.46	75.46	75.47	75.47
$\Delta T_{ONB}$	1.01	0.98	1.01	0.99	1.03	1.00
T <sub>wl</sub>	76.48	76.44	76.47	76.45	76.50	76.47
$\Delta T_{wall}$	7.07	5.91	7.06	6.04	7.2	6.06
$\delta$ (mm)	1.27	1.14	1.255	1.136	1.249	1.122

## 5. Assessment of wall thickness using single phase data

For single phase data the following four experimental data were selected (see Table 13):

**Table 13** Average  $q_s$ ,  $q_v$ , nominal  $\Delta T$  across the wall, wall conductivity and outside measured temperature ( $^{\circ}\text{C}$ ) single phase regime

$q_s$ , $\text{kW m}^{-2}$	$q_v$ , $\text{kW m}^{-3}$	$\Delta T_0$ K	K, W/mk	T <sub>w01</sub>	T <sub>w02</sub>	T <sub>w03</sub>	T <sub>w04</sub>	T <sub>w05</sub>	T <sub>w06</sub>
<b>151.57</b>	102210	6.21	13.800	80.92	77.15	79.28	75.35	77.42	73.72
<b>154.78</b>	104380	6.34	13.801	82.24	78.43	80.69	76.56	78.76	74.94
<b>156.49</b>	105530	6.41	13.802	82.96	79.10	81.40	77.42	79.53	75.61
<b>158.12</b>	106630	6.48	13.802	83.68	79.72	81.86	77.98	80.12	76.11

It is assumed that for the above range of heat fluxes, the heat flux has little effect of the local heat transfer coefficient. In order to assess the local heat transfer coefficient, an average inside wall temperature is calculated between opposite TC. The local bulk fluid temperatures are calculated based on the measurements of RTD located at the inlet and outlet of the test section as follows:

$$T_z = T_{in} + \frac{T_{out} - T_{in}}{L_h} z \quad (17)$$

From the correlation:

$$q_{sloc} = h(T_{wlloc} - T_f) \quad (18)$$

and using the estimated inside wall temperatures calculated based on nominal temperature drop,  $q_{sloc}$  is calculated and is tabulated below (Table 14):

**Table 14** Estimated local heat flux

$q_{savg}$ $\text{kW m}^{-2}$	Local surface heat flux $q_s$ ( $\text{kW m}^{-2}$ )					
	TC1	TC2	TC3	TC4	TC5	TC6
151.57	159.69	143.40	159.97	143.12	159.45	143.69
154.78	162.98	146.53	163.60	145.91	162.90	146.65
156.49	164.85	148.12	165.01	147.96	164.84	148.13
158.12	166.73	149.51	166.49	149.75	166.69	149.51

Using equation (7), and the local surface heat flux and assuming that  $q_v$  is constant regardless of the location, one may calculate the local wall thickness (Table 15):

**Table 15** Estimated local wall thickness after first iteration

$q_{savg}$	Wall thickness (mm)
------------	---------------------

$\text{kWm}^{-2}$	TC1	TC2	TC3	TC4	TC5	TC6
151.57	1.283	1.152	1.285	1.150	1.281	1.154
154.78	1.282	1.153	1.287	1.148	1.281	1.154
156.49	1.283	1.152	1.284	1.151	1.282	1.152
158.12	1.284	1.151	1.282	1.153	1.283	1.151

With the new wall thickness, the iterative process described above is repeated until the wall thickness for two consecutive iterations became very close. Table 16 summarizes wall thickness obtained at subsequent iterations until convergence is reached:

**Table 16** Local wall thickness (mm) at subsequent iterations

TC1	TC2	TC3	TC4	TC5	TC6
Third iteration					
1.268	1.167	1.270	1.166	1.266	1.169
1.267	1.178	1.271	1.171	1.268	1.179
1.266	1.167	1.267	1.166	1.267	1.168
1.270	1.168	1.266	1.169	1.268	1.166
Fourth iteration					
1.263	1.170	1.266	1.169	1.262	1.172
1.263	1.171	1.267	1.165	1.264	1.172
1.262	1.169	1.263	1.168	1.263	1.170
1.265	1.170	1.262	1.171	1.264	1.168
Fifth iteration					
1.265	1.170	1.268	1.169	1.263	1.172
1.265	1.171	1.268	1.165	1.266	1.172
1.264	1.169	1.265	1.168	1.265	1.170
1.267	1.170	1.263	1.171	1.265	1.168

One can notice that the fourth and fifth iterations are reasonably close; therefore the final result is taken by averaging wall thickness values from the fifth iteration.

## 6. Direct measurements

Direct measurement of the wall thickness was performed using an electronic caliper having 0.01 mm accuracy. In order to obtain a better estimate of the wall thickness, the measurement were repeated seven times and averaged. They are presented in Table 17:

**Table 17** Results of wall thickness measurement (mm) using an electronic caliper

Location	Measurement #							Average (mm)
	1	2	3	4	5	6	7	
TC1-3-5	1.26	1.25	1.25	1.24	1.26	1.25	1.25	<b>1.25</b>
TC2-4-6	1.17	1.18	1.17	1.18	1.17	1.17	1.19	<b>1.18</b>

In addition to the caliper measurement, a photographic method was also employed. A 15 mm long slice of the test section was cut, the edges chamfered and several photos ( see Figure 4) were taken

with a Sony DSC H2 digital camera. The resolution was set at 6 MP. The clearest photos were magnified, and digitally processed to enhance the contrast and printed. Wall thickness measurements were performed with an electronic caliper (0.01 mm accuracy) on the printed photos. The blue marks in Figure 4 represent thermocouple locations. Although a ruler was included in the picture, the scaling was based on the outside diameter of the test section ( $D_o=8.020$  mm), which was measured with a mechanical caliper having 0.0013 mm accuracy. The results of the photographic measurement are shown in Table 18, along with a summary of the results obtained with all the other previously-described methods:

**Table 18** Summary of wall thickness estimation

Method	Wall thickness (mm)		Observations
	Avg(1-3-5)	Avg(2-4-6)	
Direct (caliper)	1.250	1.180	Precision limited to 3 significant digits (depending on the caliper accuracy) Cannot be used in the middle of test section.
Photographic	1.240	1.140	Affected by optical distortions, smooth edges and scaling errors Cannot be used in the middle of test section
Single phase	1.265	1.170	Slow convergence, seems less accurate than boiling methods.
ONB	1.258	1.133	Fastest convergence. For the even side of test section (low heat flux) is difficult to determine with acceptable accuracy the ONB. Because of weak dependence of wall superheat on heat flux, this method may be more suitable for irregular geometries than other methods
Nucleate boiling	1.261	1.174	Moderate convergence, good accuracy.

## 7. Conclusions

1. The proposed method can be a valuable tool for determining the circumferential heat flux variation in directly heated tubes, cooled internally or externally as is done frequently in thermalhydraulic studies employing tubes as fuel element simulators.
2. The proposed method will also provide confirmation for mechanical, ultrasonic or photographically based wall thickness measurement methods, and may well be more accurate than these conventional method.
3. The method is based on the principle that for directly heated tubes, cooled internally, the single phase heat transfer coefficient (or the wall superheat in nucleate boiling or at ONB) is uniform around the circumference and is therefore independent of the variation in wall thickness.
4. This method is applied to a R-134a cooled tube. After careful calibration of the surface thermocouples located on the insulated side of the test section, the inside wall temperature is evaluated using the simple Fourier equation applied to a directly heated annulus. The variation in surface heat flux to the coolant is also evaluated.
5. The three analytical methods for evaluating the wall thickness variation (based on (i) single phase heat transfer data (ii) nucleate boiling data and (iii) ONB data) have been compared to two direct methods (direct caliper measurements, and photographic-based measurements). The agreement between these five methods is good.

6. The direct measurements confirm that the proposed analytical methods are an accurate method for determining the circumferential wall thickness variation.
7. The proposed methods are thought to be especially valuable for thermalhydraulic studies where a nominally uniform wall thickness can have a variation of  $\pm 5\%$  and will results in a similar variation in surface heat flux. A more accurate knowledge of the actual circumferential wall thickness will permit for a more precise measurement of CHF and PDO heat transfer coefficient.

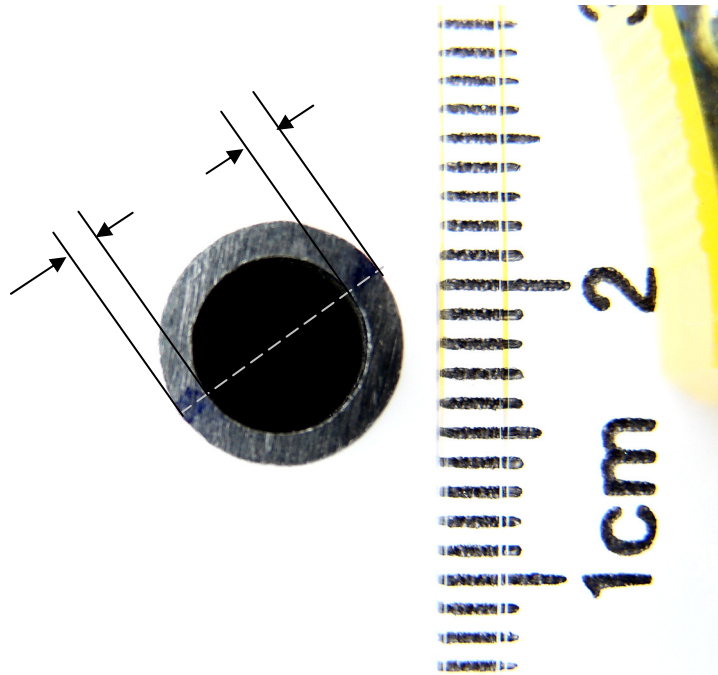


**Figure 4** Magnified photo of the end of the test section

## 8. References

- [1] Corsan, J.M., Budd, J.N., and Hemminger, W.F., An intercomparison involving PTB and NPL of thermal conductivity measurements on stainless steel, Inconel and Nimonic alloy reference materials, and an iron alloy, 12<sup>th</sup> European Conference on Thermophysical Properties, Vienna, Austria, 1990
- [2] Davis, E.J., Anderson, G.H., The incipience of nucleate boiling in forced convection flow, AIChE Journal 12 (4), 774–780, 1966.
- [3] Incropera, F.P. and DeWitt, D.P., Fundamentals of Heat and Mass Transfer, Fourth edition, 1996.
- [4] National Instruments – Measurement and Automation Catalogue, 1999.

- [5] Tavoularis, S., Measurements in Fluid Mechanics, Cambridge University press, 2005.